

LETTER TO THE EDITOR

**Charge localization and phonon spectra in hole-doped
La₂NiO₄**R J McQueeney[†], A R Bishop[†], Ya-Sha Yi[†] and Z G Yu[‡][†] Los Alamos National Laboratory, Los Alamos, NM 87545, USA[‡] Department of Chemistry, Iowa State University, Ames, IA 50011, USA

Received 23 March 2000

Abstract. The in-plane oxygen vibrations in La₂NiO₄ are investigated for several hole-doping concentrations both theoretically and experimentally via inelastic neutron scattering. Using an inhomogeneous Hartree–Fock plus random-phase approximation numerical method in a two-dimensional Peierls–Hubbard model, it is found that the doping induces stripe ordering of localized charges, and that the strong electron–lattice coupling causes the in-plane oxygen modes to split into two subbands. This result agrees with the phonon band splitting observed by inelastic neutron scattering in La_{2–x}Sr_xNiO₄. Predictions of strong electron–lattice coupling in La₂NiO₄, the proximity of both oxygen-centred and nickel-centred charge ordering, and the relation between charged stripe ordering and the splitting of the in-plane phonon band upon doping are emphasized.

There is currently great interest in the importance of charge localization and ordering tendencies in a variety of doped transition metal oxides, including nickelates, bismuthates, cuprates, and manganites [1–7]. Recent experiments have suggested nanoscale coexistence of charge and spin ordering, as well as related multiscale dynamics [1–10]. The cuprates have been widely investigated, both theoretically and experimentally, as this inhomogeneity may be related to high-temperature superconductivity [11–18].

The nickelates are considered strong electron–lattice (e–l) coupling systems, which helps stabilize charge ordering in the form of ‘stripe’ phases [19,20]. For the commensurate $\frac{1}{3}$ -doping case of La_{1.67}Sr_{0.33}NiO₄, it has been shown in optical absorption and Raman scattering experiments that new phonon modes appear when the temperature is lowered below the stripe-ordering temperature ($T_{so} = 240$ K); this is a signature of the stripe formation [8–10]. Until now, only the temperature dependence and the apical oxygen (Ni–O(2)) vibrations have been investigated. However, the doping dependence and the in-plane oxygen vibrations (Ni–O(1) stretching modes) are also very important for the properties of the quasi-two-dimensional nickelate materials. In this study, we use an inhomogeneous Hartree–Fock (HF) plus random-phase approximation (RPA) numerical method for a two-dimensional (2D), four-band Peierls–Hubbard model to interpret the inelastic neutron scattering spectra. This reveals specific signatures of the stripe patterns in the in-plane oxygen phonons.

Our main results are:

- (i) There is agreement between the results from our multiband model including electron–electron and e–l interactions and the inelastic neutron scattering spectra for the in-plane oxygen vibrations with various commensurate hole-doping concentrations.
- (ii) The theoretical results predict new vibrational modes (‘edge modes’) which are associated with oxygen motions near localized holes or in the vicinity of stripes.

- (iii) The e-l coupling strength at which the best agreement between our model and the inelastic neutron scattering data is achieved is close to the predicted transition from an oxygen-centred stripe phase to a nickel-centred one. This suggests that the nickelates may be in a mixed state of both stripe phases, and sensitive to temperature, pressure, and magnetic field.

The inelastic neutron scattering spectra were measured for polycrystalline $\text{La}_{2-x}\text{Sr}_x\text{NiO}_4$ for various doping concentrations, $x = 0, 1/8, 1/4, 1/3, 1/2$. Time-of-flight neutron scattering measurements were performed on the Low Resolution Medium Energy Chopper Spectrometer at Argonne National Laboratory's Intense Pulsed Neutron Source. For all measurements, an incident neutron energy of 120 meV was chosen and data were summed over all scattering angles from 2° to 120° . Detailed information on the experiment, as well as the preparation of the samples used, can be found in reference [21]. The focus is on the (neutron-scattering-weighted) generalized density of states (GDOS) of phonons and particular attention is given to the in-plane oxygen vibrations, i.e., the Ni-O(1) stretch modes.

Figure 1 shows the experimental GDOS for several hole concentrations at $T = 10$ K for phonon modes in the range from 50–100 meV. From the analysis of lattice dynamical shell-

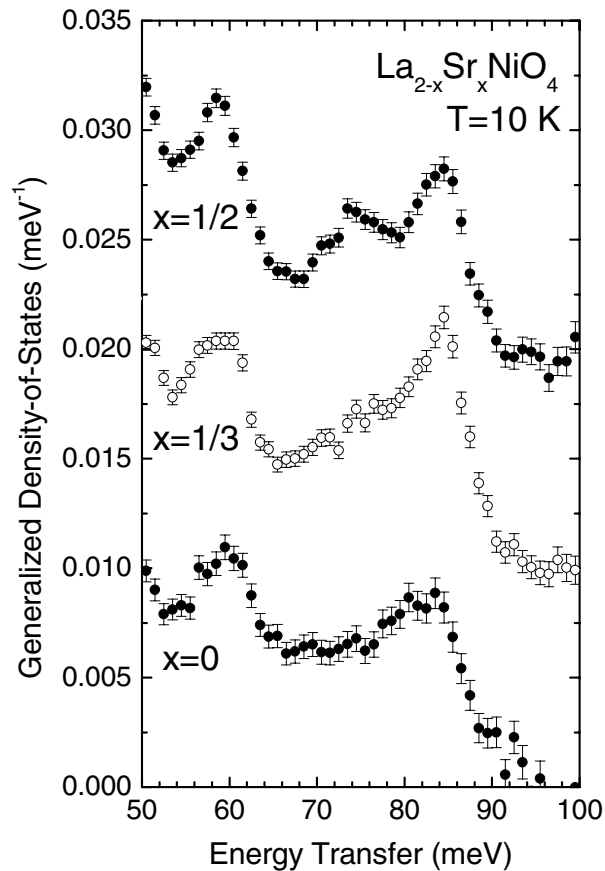


Figure 1. The generalized phonon density of states for three concentrations of $\text{La}_{2-x}\text{Sr}_x\text{NiO}_4$. The frequency region shown (above 65 meV) consists of in-plane polarized oxygen modes (breathing modes) which are well separated from other types of phonon. Data are offset vertically for clarity.

model calculations, it is known that the in-plane Ni–O(1) oxygen stretch modes are separated in frequency from other vibrations, and the phonon intensity above 65 meV is associated entirely with these vibrations. For the low-doping samples ($x = 1/8$ and $1/4$, not shown), there is little change in the ~ 81 meV phonon band [21], but for the $x = 1/3$ and $x = 1/2$ samples, a new peak appears around 75 meV along with a slight hardening of the main band. This feature is interpreted as a splitting of the 81 meV Ni–O(1) stretching band into two phonon bands centred at approximately 83 meV and 75 meV.

In order to understand this dependence of the Ni–O(1) stretching modes on hole concentration and its possible reflection of stripe ordering, we have performed a calculation of the phonon spectrum in a minimal Peierls–Hubbard model in 2D. Due to the strong e–l coupling expected in the nickelates, we choose to model with an inhomogeneous HF plus RPA numerical approach [22–24]. This has proven to be a very robust method for studying charge localization and stripe formation, especially when electron–lattice coupling is strong, obviating subtle many-body effects and quantum fluctuations [25].

We use a 2D four-band extended Peierls–Hubbard model of a doped NiO₂ plane, which includes both electron–electron and e–l interactions [23, 24]. Here, for nickelates, besides the $d_{x^2-y^2}$ orbital used in the cuprate models [23], the d_{3z^2-1} Ni d orbitals must be included to account for the higher spin state ($S = 1$) at half-filling (i.e. undoped). Our model Hamiltonian is [25]

$$H = \sum_{(ij),m,n,\sigma} t_{im,jn}(u_{ij})(c_{im\sigma}^\dagger c_{jn\sigma} + \text{H.c.}) + \sum_{i,m,\sigma} \epsilon_m c_{im\sigma}^\dagger c_{im\sigma} + \sum_{(ij)} \frac{1}{2} K_{ij} u_{ij}^2 + H_c \quad (1)$$

where $c_{im\sigma}^\dagger$ creates a hole with spin σ at site i in orbital m (Ni $d_{x^2-y^2}$, d_{3z^2-1} , or O p). The Ni–O hopping $t_{im,jn}$ has two values: t_{pd} between $d_{x^2-y^2}$ and p and $\pm t_{pd}/\sqrt{3}$ between d_{3z^2-1} and p. The O-site electronic energy is ϵ_p , and the Ni-site energies are ϵ_d and $\epsilon_d + E_z$ for ϵ_m , with E_z the crystal-field splitting on the Ni site. H_c describes the electron correlations in the Ni orbitals:

$$H_c = \sum_{im} (U + 2J) n_{im\uparrow} n_{im\downarrow} - \sum_{i,m \neq n} 2J \mathbf{S}_{im} \cdot \mathbf{S}_{in} + \sum_{i,m \neq n,\sigma,\sigma'} (U - J/2) n_{im\sigma} n_{in\sigma'} \\ + \sum_{i,m,n} J c_{im\uparrow}^\dagger c_{im\downarrow}^\dagger c_{in\downarrow} c_{in\uparrow}. \quad (2)$$

The electron–electron interactions include the on-site Ni Coulomb repulsions (U) as well as the Hund interaction (J) at the same Ni site to account for the high-spin situation. (The interplay of the two orbitals can also lead to pseudo-Jahn–Teller distortions [25], but these are not our focus here.) We emphasize that, due to the large spin at the nickel site, Hund’s rule leads to ferromagnetic exchange coupling $-2J$, and $\mathbf{S}_{im} = \frac{1}{2} \sum_{\tau\tau'} c_{im\tau}^\dagger \boldsymbol{\sigma}_{\tau\tau'} c_{im,\tau'}$, with $\boldsymbol{\sigma}$ the Pauli matrix. For the e–l interaction, we assume that the Ni–O hopping is modified linearly by the O-ion displacement $u_{ij} = u_O$ as $t_{im,jn}(u_{ij}) = t_{im,jn}(1 \pm \alpha u_O)$, where the + (–) applies if the bond shrinks (stretches) with positive u_O . For the lattice terms, we study only the motion of O ions along the Ni–O bonds—other oxygen (or Ni) distortion modes can readily be included if necessary. It is known that for the nickelates the e–l coupling is stronger than in cuprates [19, 20], and is therefore likely to play an even more decisive role in the formation, localization, and nature of stripe phases. We adopt the following representative parameters for the nickelate materials [20]: $t_{pd} = 1$, $\Delta = \epsilon_p - \epsilon_d = 9$, $U = 4$, $J = 1$, $E_z = 1$, and $K = 32t_{pd}/\text{\AA}^2$ (all in units of t_{pd}). In real oxides [20, 26], t_{pd} is estimated to be in the range 1.3 eV–1.5 eV. The electron–lattice coupling strength is varied to achieve a best fit to the neutron scattering data; we find $\alpha \approx 3.0$. The commensurate doping cases are examined in a

4×4 unit supercell for $x = 0, 1/2$ and a 3×3 unit supercell for $x = 1/3$. Periodic boundary conditions are used.

The densities of states (DOS) of in-plane phonons were calculated from our model at $x = 0, 1/3, 1/2$ and are shown in figure 2. For the undoped case, as the ground state is spatially homogeneous, only one oxygen phonon band appears, centred around 80.5 meV. When holes are added into the NiO_2 plane at $x = 1/3$, the ground state is found to be a stripe pattern with more holes accumulating along the $(1, 1, 0)$ direction, forming an antiphase domain wall within the original antiferromagnetic background. This is consistent with many neutron, optical, and Raman scattering experiments [4, 8–10]. Interestingly, we find that a new phonon band appears centred at 75 meV. In addition, there is a hardening of the main phonon band (to 83 meV) corresponding to an overall splitting of 8 meV. From examination of the eigenvectors, the main character of this band is local oxygen vibrations in the vicinity of the stripe, i.e. having the nature of localized ‘edge modes’ (see [25] for more details). For the higher doping $x = 1/2$, the charge ordering takes on a commensurate checkerboard pattern. A similar splitting of the 85 meV phonon band into two phonon bands around 83 and 75 meV is again found. At this half-doping, the checkerboard ground state is in essence a commensurate charge-density-wave (CDW) system with the nature of an ordered binary alloy.

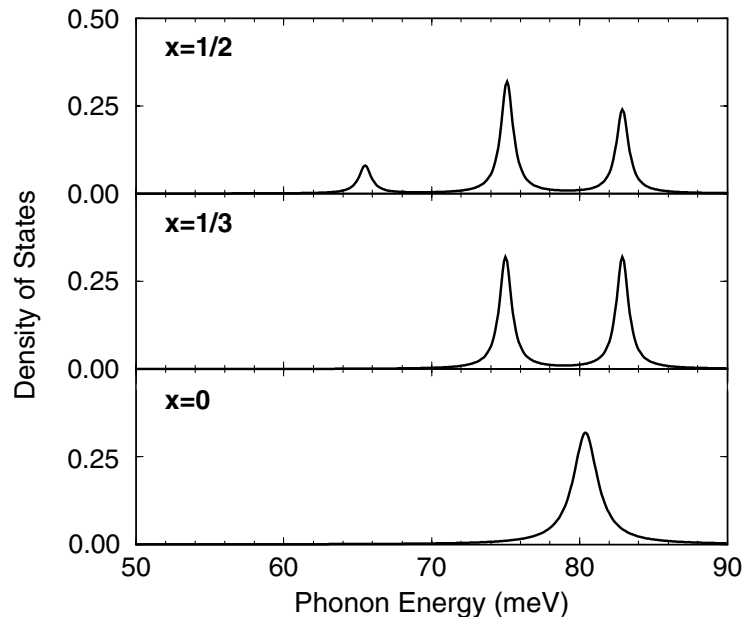


Figure 2. The calculated densities of states of the oxygen breathing modes for various doping concentrations. The results have been broadened with a Lorentzian of width 2 meV for $x = 0$ and 1 meV for $x = 1/3$ and $1/2$. The electron–lattice coupling constant used is $\alpha = 3.0$.

The above results are in agreement with the GDOS data obtained from inelastic neutron scattering, which are shown in figure 1. In addition to the splitting energy, even the slight hardening of the main band observed experimentally is accounted for in the model. Besides the new phonon modes centred at 75 meV appearing for the $1/3$ and $1/2$ doping, another low-intensity phonon mode around 65 meV is also predicted in our model at $x = 1/2$ (figure 2). The signatures for these modes are weak, however, so they may be difficult to detect in the current experiment. In so far as we have included only a small subset of the possible oxygen

displacement patterns and wavevectors in the model (whereas the neutron scattering experiment samples all wavevectors and polarizations), the relative intensities and widths of the bands obtained by experiment and theory cannot be usefully compared.

We emphasize that the excellent agreement between our model and the GDOS experimental data is achieved by varying the e–l coupling strength to match the positions of the phonon bands. As noted, the choice of $\alpha \approx 3$ best fits the data; our model calculations predict a variation of the phonon splitting with α which is quite large ($\Delta\omega_{split}/\Delta\alpha \approx 7$ meV). Most strikingly, as illustrated in figure 3, an O-centred stripe is found as the ground state at small $\alpha \lesssim 2.2$, while for a larger $\alpha \gtrsim 3.0$, a Ni-centred stripe is found as the ground state [25]. The transition region includes $\alpha \approx 3.0$, where the best agreement between figure 2 based on our model and figure 1 based on the inelastic neutron scattering spectra is achieved. It has been suggested from various experimental data that stripe formation for $x = 1/3$ cannot be simply assigned as Ni centred or O centred [19], but is also dependent on temperature. Our comparison of theory and experiment provides a possible explanation for the sensitivity of stripe formation; it suggests that $\text{La}_{1.67}\text{Sr}_{0.33}\text{NiO}_4$ may be in a mixed-stripe-phase state, and also in a region of sensitivity to temperature, pressure, magnetic field, etc.

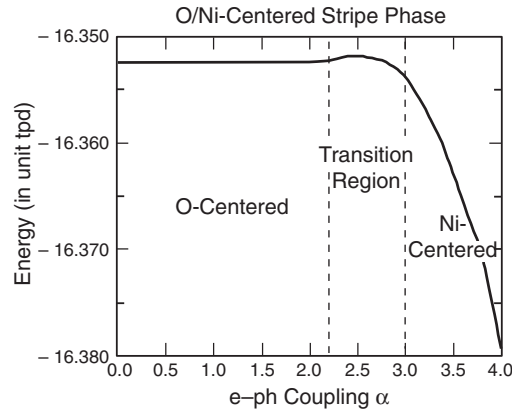


Figure 3. The energy dependence on the electron–lattice coupling α for the $\frac{1}{3}$ -doped nickelates (solid line). For $\alpha \leq 2.2$, the ground state is in an O-centred stripe phase, while for $\alpha \geq 3.0$, the Ni-centred state is found as the ground state. The sensitive transition region is from $\alpha = 2.2$ to $\alpha = 3.0$.

In conclusion, we have made a study of oxygen breathing lattice vibrations in $\text{La}_{2-x}\text{Sr}_x\text{NiO}_4$ via inelastic neutron scattering compared with predictions of a 2D four-band model, including both electron–lattice and electron–electron interactions. The in-plane oxygen vibrations above 65 meV were thoroughly investigated. The splitting of the in-plane 81 meV band upon doping into two subbands centred around 75 meV and 83 meV is observed experimentally and predicted theoretically, and interpreted in terms of new localized phonon modes (‘edge modes’ at charge-localized stripes). The excellent agreement between the experiment and the model strongly supports the view that strong electron–lattice coupling in this kind of material plays a decisive role in the charge localization and mesoscopic stripe formation. For the doping at $x = 1/3$, at which stripes are found both in experiments and our model, our results suggest that there may be a mixed state of O- and Ni-centred stripe phases, and sensitivity to temperature, pressure, and magnetic field. Our model calculations also predict distinctive dispersion of the phonon bands, as well as inhomogeneous magnetoelastic coupling along the boundaries between charge-rich and magnetic nanophase domains [25].

These predictions require additional experiments for their confirmation and to investigate their consequences.

We have benefited from valuable discussions with Dr J T Gammel. This work was supported (in part) by the US Department of Energy under contract W-7405-Eng-36 with the University of California. This work has benefited from the use of the Intense Pulsed Neutron Source at Argonne National Laboratory. This facility is funded by the US Department of Energy, BES–Materials Science, under contract W-31-109-Eng-38.

References

- [1] Tranquada J M, Buttrey D J, Sachan V and Lorenzo J E 1994 *Phys. Rev. Lett.* **73** 1003
- [2] Tranquada J M *et al* 1996 *Phys. Rev. B* **54** 7489
- [3] Chen C H, Cheong S-W and Cooper A S 1994 *Phys. Rev. Lett.* **71** 2461
- [4] Cheong S-W *et al* 1994 *Phys. Rev. B* **49** 7088
Lee S-H and Cheong S-W 1997 *Phys. Rev. Lett.* **79** 2514
- [5] Nakajima K *et al* 1997 *J. Phys. Soc. Japan* **66** 809
- [6] Tranquada J M *et al* 1995 *Nature* **375** 561
Tranquada J M, Axe J D, Ichikawa N, Moodenbaugh A R, Nakamura Y and Uchida S 1997 *Phys. Rev. Lett.* **78** 338
- [7] Ramirez A P 1997 *J. Phys.: Condens. Matter* **9** 8171
- [8] Blumberg G, Klein M V and Cheong S-W 1998 *Phys. Rev. Lett.* **80** 564
- [9] Katsufuji T, Tanabe T, Ishikawa T, Fukuda Y, Arima T and Tokura Y 1996 *Phys. Rev. B* **54** R14 320
- [10] Yamamoto K, Katsufuji T, Tanabe T and Tokura Y 1998 *Phys. Rev. Lett.* **80** 1493
- [11] Zaanen J and Gunnarsson O 1989 *Phys. Rev. B* **40** 7391
Poilblanc D and Rice T M 1989 *Phys. Rev. B* **39** 9749
Schulz H J 1989 *J. Physique* **50** 2833
Machida K 1989 *Physica C* **158** 192
Kata K, Machida K, Nakanishi H and Fujita M 1990 *J. Phys. Soc. Japan* **59** 1047
Verges J A *et al* 1991 *Phys. Rev. B* **43** 6099
Inui M and Littlewood P B 1991 *Phys. Rev. B* **44** 4415
Zaanen J and Oles A M 1996 *Ann. Phys., Lpz.* **5** 224
- [12] Emery V J and Kivelson S A 1993 *Physica C* **209** 597
- [13] Emery V J and Kivelson S A 1995 *Nature* **374** 434
- [14] Castro Neto A H and Hone D 1996 *Phys. Rev. Lett.* **76** 2165
- [15] White S R and Scalapino D J 1999 *Phys. Rev. B* **60** R753
White S R and Scalapino D J 1997 *Phys. Rev. B* **55** R14701
- [16] Krotov Yu A, Lee D H and Balatsky A V 1997 *Phys. Rev. B* **56** 8367
- [17] Zaanen J, Horbach M L and van Saarloos W 1996 *Phys. Rev. B* **53** 8671
- [18] Bianconi A *et al* 1996 *Phys. Rev. Lett.* **76** 3412
- [19] Wochner P, Tranquada J M, Buttrey D J and Sachan V 1998 *Phys. Rev. B* **57** 1066
- [20] Zaanen J and Littlewood P B 1994 *Phys. Rev. B* **50** 7222
- [21] McQueeney R J, Sarrao J L and Osborn R 1999 *Phys. Rev. B* **60** 80
- [22] Batistic I and Bishop A R 1992 *Phys. Rev. B* **45** 5282
- [23] Yonemitsu K, Bishop A R and Lorenzana J 1992 *Phys. Rev. Lett.* **69** 965
- [24] Yonemitsu K, Bishop A R and Lorenzana J 1993 *Phys. Rev. B* **47** 12 059
- [25] Yi Ya-Sha, Yu Z G, Bishop A R and Gammel J T 1998 *Phys. Rev. B* **58** 503
- [26] van Elp J, Kuiper P and Sawatzky G A 1992 *Phys. Rev. B* **45** 1612